Silva Fennica vol. 59 no. 1 article id 24027
Category: research note
https://doi.org/10.14214/sf.24027
SILVA FENNICA
http://www.silvafennica.fi
ISSN-L 0037-5330 | ISSN 2242-4075 (Online)
The Finnish Society of Forest Science

Julian Frey[1], Zoe Schindler[1], Patrick McClatchy[1], Christopher Morhart[1], Elena Larysch[1] and Thomas Seifert[1,2]

The 3D reconstruction of wood and leaves from terrestrial laser scanning – a case study on PAR measurements below a solitary *Malus domestica* tree

Frey J., Schindler Z., McClatchy P., Morhart C., Larysch E., Seifert T. (2025). The 3D reconstruction of wood and leaves from terrestrial laser scanning – a case study on PAR measurements below a solitary *Malus domestica* tree. Silva Fennica vol. 59 no. 1 article id 24027. 15 p. https://doi.org/10.14214/sf.24027

Highlights

- Direct reconstruction of leaf and wood polygons from terrestrial laser scanning data by open source software.
- Validation of reconstruction based on in-situ PAR measurements and direct comparison to a turbid voxel approach.
- High correlations between in situ PAR measurements and RTM simulation (r = 0.92).

Abstract

In this paper, we present a new methodology that directly extracts the geometry of woody features (wood and bark) and foliage from 3D data originating from terrestrial laser scans. Our goal was to enhance the precision of radiative transfer models for modelling tree shading by using highly resolved 3D tree models. The approach was tested on a single apple tree (*Malus domestica* (Suckow) Borkh.) in a peri-urban setting and was validated by utilising an open-source radiative transfer model and comparing the simulation output with in-situ measurements of photosynthetically active radiation (PAR) as well as simulations utilizing turbid voxels of 0.2 m and 1 m edge length. The in-situ measurements of 60 PAR sensors showed a correlation coefficient (r) of 0.92 with the simulated light intensities for the reconstructed polygons which was higher than for the voxel-based approaches (0.2 m: r = 0.85, 1 m: r = 0.73). We were able to demonstrate that our approach effectively simulates light extinction through the canopy. This innovative method has the potential to easily provide detailed insights into high resolution radiation patterns within forests, which are connected to multiple ecosystem functions like species and habitat diversity.

Keywords leaf geometry; LESS; light modelling; *Malus domestica*; PAR; structural tree model; terrestrial laser scanning
Addresses [1]Chair of Forest Growth and Dendroecology, University of Freiburg, Freiburg im Breisgau, Tennenbacher Str. 4, 79106 Freiburg, Germany; [2]Department of Forest and Wood Science, Stellenbosch University, Private Bag X1, Matieland, 7602, Stellenbosch, South Africa
E-mail julian.frey@wwd.uni-freiburg.de
Received 2 May 2024 **Revised** 27 January 2025 **Accepted** 28 January 2025

1 Introduction

Solar radiation is an essential driver of tree growth and controls tree development (Leuchner et al. 2012). For a deeper understanding of how solar radiation interacts with both the Earth's atmosphere and biosphere, radiative transfer modelling (RTM) has been proven to be an important tool (Chen et al. 2008; Ni-Meister and Gao 2011; Widlowski et al. 2014; Magney et al. 2016; Li et al. 2018; Porcar-Castell et al. 2021). RTMs can offer valuable insights into a wide range of environmental phenomena by simulating the absorption, scattering, and reflection of light by various materials and surfaces. Particularly in the field of forest ecology, these models help to understand how solar radiation interacts with the forest canopy, ultimately impacting the energy balance of the ecosystem (Brunner 1998; Meister and Gao 2011; Ligot et al. 2014; Ni-Meister and Gao 2021; Regaieg et al. 2021; Burchard-Levine et al. 2022). By providing information on the amount and distribution of energy within forests, we can study forest productivity, carbon cycling, biodiversity, and the impact of deforestation and forest fragmentation on regional climate patterns (Huston and Marland 2003; Malhi et al. 2004; Latimer and Zuckerberg 2017; Pacheco-Labrador et al. 2022; Wang and Frankenberg 2022).

Light extinction modelling, therefore, is a requirement for ecological habitat characterisation as well as for a plausible simulation of forest growth with eco-physiological process models (Van der Zande et al. 2011; Bittner et al. 2012; Leuchner et al. 2012; Lintunen et al. 2013; Forrester et al. 2019; Pacheco-Labrador et al. 2022). Since the assessment of the forest structure itself is difficult, former studies have concentrated on modelling these processes with strongly simplified representations of trees often based on conical or oval crown shapes or sandwich structures (Wang and Jarvis 1990; Rötzer et al. 2012; Vezy et al. 2018). During the last decade, light models based on terrestrial laser scanning (TLS) voxel shapes have been established and tested, but first studies either lack ground truth data or were completely based on simulated forest stands (Van der Zande et al. 2010, 2011). Cifuentes et al. (2017) presented an elaborate voxel-based model and applied it to real forest stands scanned with a phase shift TLS device. The model results showed relatively poor correlations with measured photosynthetically active radiation (PAR) values. The authors discuss that this might be caused by occlusion effects from the phase shift TLS system and improvable classifications of leaves and branches (Cifuentes et al. 2017).

Kükenbrink et al. (2019) modelled the irradiance field of a single tree (*Tilia cordata* Mill.) on a flat meadow and conducted field spectroradiometer measurements along transects pointing in an angular grid away from the trunk. They simulated the scene using the DART model (discrete anisotropic radiative transfer model, Gastellu-Etchegorry et al. 2012; Gastellu-Etchegorry et al. 2017; Malenovský et al. 2021) with the crown space represented as small voxels (0.25 m) of a turbid medium with associated leaf spectrum, plant area density (PAD) and a leaf angle distribution to each voxel. Their modelling approach was able to simulate and predict the interactions of radiation with the canopy in high spectral and spatial resolution.

Calders et al. (2018) presented a workflow that used highly detailed leaf-off TLS data to generate a virtual forest. Their approach modelled the structure of single trees from automatic segmentation and added leaf polygons afterwards (Calders et al. 2018; Xie et al. 2018; Liu et al. 2022). Leaf optical properties were added to the leaves based on field measurements of leaf spectra on the site for the respective tree species. They achieved good agreement between digital and simulated hemispherical photographs. Nevertheless, this approach requires leaf off conditions for scanning, introducing large time lags between the scan and the leaf-on conditions, which makes a comparison difficult due to possible changes in the ecosystem. Additionally, the structural modelling of trees from laser-scan-based point clouds is prone to errors (Morhart et al. 2024), and the

addition of simulated leaves depends on various parameters that are species-specific and need to be optimised (Rosskopf et al. 2017).

A similar approach was followed by Janoutová et al. (2019) who generated detailed 3D representations of Norway spruce (*Picea abies* (L.) H. Karst.) trees from an automatically generated wood skeleton and attached 3D representations of shots. These realistic tree models were used in the DART model to evaluate the effects of canopy structural complexity on forest reflectance. Four scenarios with increasing structural detail were simulated, ranging from simple geometric shapes filled with turbid media to detailed models incorporating individual needle shoots. The results showed that while all scenarios approximated observed reflectance, models with detailed structures better matched airborne and Sentinel-2 remote sensing data. This model was later adapted to broadleaved trees (Janoutová et al. 2021).

Kükenbrink et al. (2021) also used TLS to model radiative transfer in two forest plots. Contrasting to Calders et al. (2018), they scanned the forests during leaf-on conditions. After leaf-wood separation, they simulated the optical properties of the foliage as turbid voxels based on the plant area density at each voxel. They were able to mimic a realistic light extinction through the canopy. The trade-off of this approach is that the voxels add a layer of spatial uncertainty, and the calculation of the PAD and the radiative transfer through the turbid voxels is computationally demanding and errors from the PAD estimation propagate through the radiative transfer model. Nevertheless, Janoutová et al. (2019) found slightly better representation of the canopy reflectance for a turbid voxel approach for needles with a mesh representation of the woody materials, compared to a mesh representation of the needles in a spruce stand. It is currently not clear which modelling approach, explicitly geometric or voxel-based, leads to the best representation of the simulated light for broadleaved trees according to the spatial, temporal and spectral dimension, since a better spatial representation does not necessarily lead to a better spectral representation of the radiative transfer (e.g. Schneider et al. 2014).

In this paper, we introduce a new approach to derive wood and leaf geometry directly from TLS data. We evaluate our approach using an open-source radiative transfer model and in-situ measurements of PAR to compare our reconstruction with a voxel-based reconstruction.

2 Methods

2.1 Research site

Our research site was based within the city of Freiburg in southwest Germany. We conducted the following methodology on a single apple tree (*Malus domestica* (Suckow) Borkh.) within a peri-urban environment (48°00′N, 07°48′E) on a flat meadow in August 2023. The tree had a diameter at breast height (DBH) of 0.19 m, a height of 6.6 m, a crown base height of 2.1 m and a crown projection area of 44.8 m^2. The weather on the acquisition day was warm, calm and sunny (mean global radiation 240 J cm^{-2} h^{-1}, mean temperature 28 °C, mean wind speed 2.0 m s^{-1}) without visible clouds. The site is about 230 m a.s.l., and no larger buildings or vegetation were nearby to influence the research tree by shadows or reflections.

2.2 TLS campaign and preprocessing

The target tree was scanned from eight positions at about 10 m distance to the stem using a RIEGL VZ-400i (RIEGL Laser Measurement Systems GmbH, Horn, Austria) with an angular resolution of 0.04° and a pulse rate of 1200 kHz. This setting was chosen as a compromise of resolution

and coverage, since closer scans increase the occlusion of the upper crown. Scan positions were recorded using an integrated GNSS system with a live correction from a base station in direct proximity. Scans were automatically co-registered on the device using a proprietary algorithm by the manufacturer, based on the point cloud, GNSS, and onboard measurements from an inertial measurement system. The successful coregistration was later on validated visually (no blur or duplication of smaller branches and a smooth stem surface). Scans were filtered for noise based on points with a very low reflectance (≤ –15 dB) and high pulse deviation (≥ 15). The filtered point clouds were combined using a 1 cm voxel grid where the centre of gravity of every voxel was calculated to exclude duplicated points from further analyses and to homogenise the point density. All preprocessing was conducted in RiSCAN software (v2.18.1, RIEGL Laser Measurement Systems GmbH, Horn, Austria).

2.3 Light measurements

To measure the PAR, we distributed 60 sensors (SQ-110, Apogee Instruments, Logan, Utah, USA) around the north side of the tree (Fig. 1). Sets of 12 sensors were grouped on 2 m × 3 m rectangular wooden structures and connected to data loggers (Adafruit Feather 32u4 Adalogger, Adafruit Industries, New York City, New York, USA). Each sensor recorded PAR at 1-minute intervals from 12:10 to 17:15 CEST. We moved one of the structures from a purely sunny position in the north-

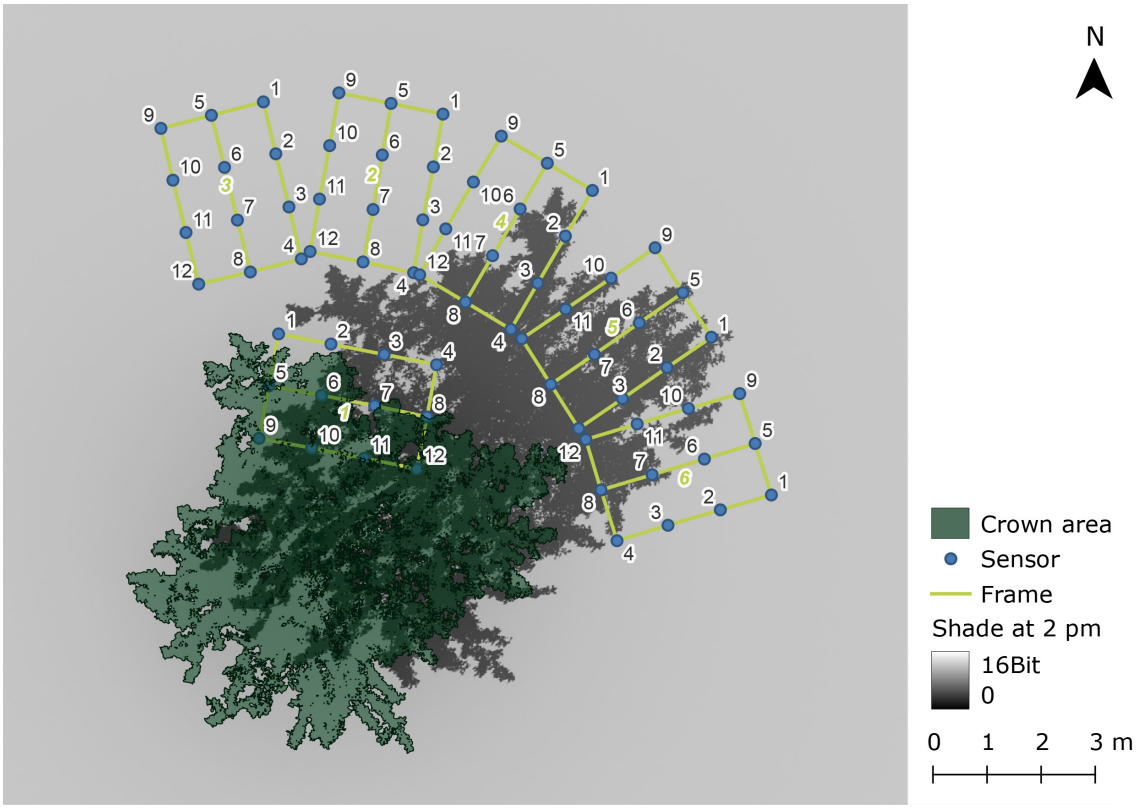

Fig. 1. Overview of the experimental setup. The green rectangles represent the wooden frames with the mounted sensors for photosynthetically active radiation (blue circles). The green numbers indicate the logger IDs, and the black numbers indicate the sensor IDs. Logger 3 was relocated and reappeared as logger 6. The dark grey area indicates the simulated shade at 2 pm. The green area shows the crown projection area of the tree.

west of the tree to the east side to capture the shade dynamics in the afternoon. The measurements from the time period when people were moving in the measurement field to move the sensors were excluded from the data. Geographic positions of the sensors were manually obtained within the TLS data to guarantee the most accurate match between TLS and sensor data.

Data of global and diffuse radiation were obtained at 5-minute intervals from a station from the German Weather Service located 3 km from the research site.

2.4 Leaf and wood polygon and voxel reconstruction

For the polygon reconstruction, the target tree was manually delineated from the point cloud using the CloudCompare software (v2.11.3, https://www.cloudcompare.org). All further processing was done in R statistical software (v4.2, R Core Team 2024). The point cloud of the tree was classified into leaf and wood points based on a reflectance threshold of –5.4 dB (Kükenbrink et al. 2021). Afterwards, all points were assigned to a voxel grid of 5 cm edge length. The 5 cm voxel resolution was chosen to ensure a sufficient amount of points in most voxels while still being smaller than a full leaf and avoiding cluster of leaves within one voxel. For each voxel, a class (leaf/wood) was assigned based on the class of the majority of the contained points. Fig. 2 illustrates the workflow to assign geometries to the voxel points. To generate polygon surfaces, all points in a voxel were projected at an optimal fitting plane, and a convex hull was spanned around this planar set of points to form a polygon. This convex hull was buffered by half of the theoretical distance between points based on the point cloud downsampling resolution (approx. 0.7 cm) to avoid gaps between the voxel cells. If there was only one or two points contained within a voxel, a six-sided polygon with a diameter of a third voxel size with the centre at the average point location and a random rotation was generated. This approach aims to resemble the original leaf area, distribution and angles as closely as possible.

To represent the foliage as turbid voxels, we utilized the AMAPvox R package (Vincent et al. 2017) developed by ”botAnique Modélisation de l’Architecture des Plantes et desvégétations”. We processed the point cloud data separated to leaf and wood points and generate two voxel datasets with Plant Area Density (PAD, m^2 m^{-3}) estimation per voxel for voxels with 0.2 and 1 m edge length (Kükenbrink et al. 2019). We limited the PAD values to a maximum of 5 m^2 m^{-3} m to avoid unlikely high values especially for the smaller voxels, since this is a known limitation of the AMAPvox approach (Weiser et al. 2021). Voxels with a PAD of zero were excluded from further analyses.

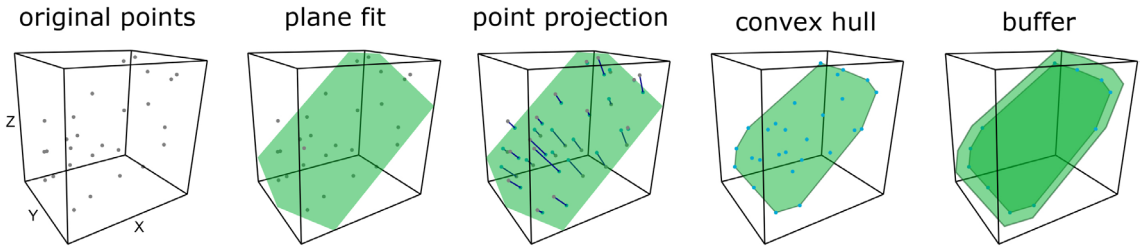

Fig. 2. Illustration of the leaf polygon geometry reconstruction workflow from light detection and ranging (LiDAR) point clouds for a single voxel. A plane is fit to the points and points are projected to the plane. The final polygon is constructed as the convex hull of the points plus a small buffer to avoid edge effects.

2.5 Radiative transfer modelling using LESS

We used LESS radiative transfer model (LargE-Scale remote sensing data and image simulation framework over heterogeneous 3D scenes, Qi et al. 2019, http://lessrt.org) to simulate the interaction of the canopy with the incoming radiation over the PAR domain (400–700 nm in 5 nm steps). Transmission and reflectance spectra for *Malus domestica* leaves were generated using the PROSPECT 4 model (Feret et al. 2008) within the implementation of the Rprospect R-package (Serbin 2013) using gap filled average leaf trait data from the TRY database (Kattge et al. 2020; Mederer et al. 2025). For all woody components a default spectrum for "bark deciduous" were exported from the DART database (Gastellu-Etchegorry et al. 2012), and for the meadow below the tree we used a meadow canopy reflectance spectra (Van Cleemput et al. 2019) from the EcoSIS database (https://ecosis.org). We generated a perfect Lambertian reflectance spectrum for the targets. We calculated suns' azimuth and elevation angles in one-minute intervals using the R package oce (Kelley and Richards 2022). Sun spectra were calculated by LESS based on the sun angles at the time of observation and the fraction of the diffuse radiation on the global radiation based on data from the closest weather service station. Since the temporal resolution of the PAR-measurements was higher (1 min) than the weather service data (10 min), we interpolated the latter based on a spline function.

Leaf and wood polygons were exported as obj-files from R either as voxel geometries or as polygons. We created three LESS simulations where we imported either the leaf-polygons, or one of the voxel geometries. We added the polygon reconstruction of the woody components to all simulations. For each of the voxels we set the PAD as it was computed by AMAPvox and the leaf angle distribution as "spherical" (Green et al. 2003). We added round white flat surfaces with 3 cm diameter below the tree at the sensor positions as targets to measure the incoming radiation. PAR-sensors were simulated as perspective cameras with a 10° opening angle 0.1 m above the targets (footprint = 2.5 cm^2) pointing downwards and emitting 12 800 rays per sensor. LESS offers a batch processing engine to iterate over simulation parameters. Since LESS can simulate only one sensor at a time we iterated over the sun positions (n = 306) and the sensor positions (n = 72) for every of the 3 reconstruction approaches resulting in more than 66 000 model runs. The measured radiation per band was converted to photon flux and summed to obtain a PAR value (Malenovský et al. 2021).

2.6 Quality assessment

We assessed the quality of the three reconstruction scenarios (vector geometry, 0.2 m and 1 m voxels) based on their overall Pearson-correlation coefficients to the PAR measurements, as well as on a single sensor basis. Scene reconstruction time and RTM runtime for the different simulations were compared.

3 Results

For the polygon reconstruction about 160 000 leaf voxels and 10 000 wood voxels were classified. A single polygon was reconstructed for every voxel. Visually, a good agreement between the scanned points and the reconstructed polygons was perceived (Fig. 3 a,b,c,d). The polygons covered a similar space as the 3D points, while the leaf angles partly differed (Fig. 3 a,b,c,d). The 0.2 m voxel reconstruction generated 6960 voxels (Fig. 3 e) with an average PAD of 2.58 $m^2\ m^{-3}$ (SD ± 1.83 $m^2\ m^{-3}$), while the 0.2 m (Fig. 3 f) reconstruction created 108 voxels with a higher aver-

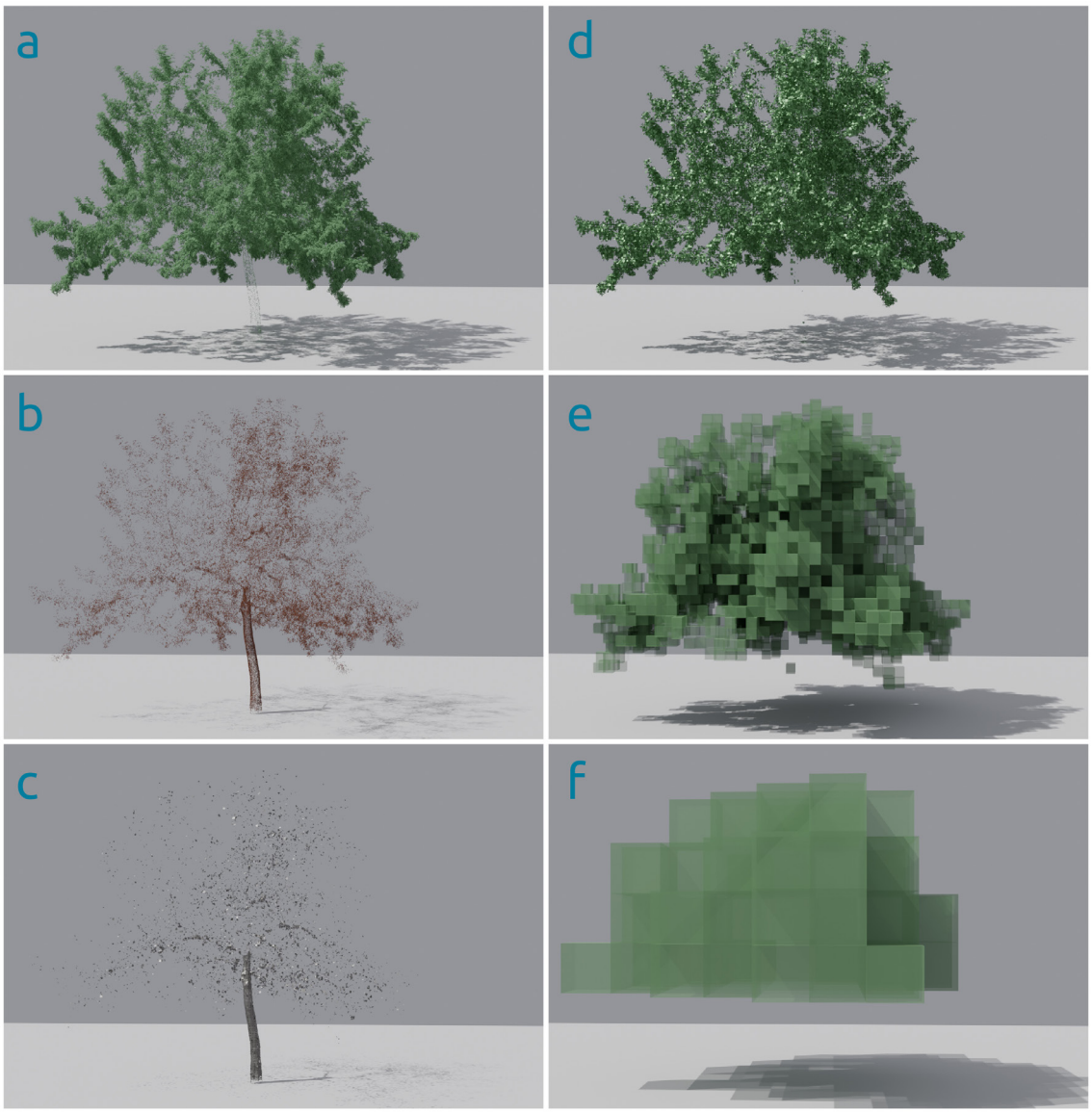

Fig. 3. Terrestrial light detection and ranging (LiDAR) Point cloud of a single *Malus domestica* tree classified as leaf (a) and wood (b) points and reconstructed polygons with simulated shade for wood (c) and leave points (d). Figures e and f illustrate the voxels for the turbid media approach in 0.2 (e) and 1 m (f) voxel resolution. Figures were generated in Blender ray tracing software for visualization purposes.

age PAD of 0.62 m^2 m^{-3} (SD ± 0.73 m^2 m^{-3}). The volume covered by the 0.2 m voxels (56 m^3) is therefore only about the half of the 1.0 m voxel reconstruction (108 m^3), but the total plant area was, even though we limited the maximum PAD per voxel, significantly higher for the 0.2 m voxel dataset (148 m^2), than for the 1.0 m voxel dataset (101 m^2). The total leaf polygon area for the polygon dataset was even higher with 187 m^2. Surprisingly, the mean simulated PAR over all sensors shows the opposite pattern with the highest average PAR for the polygon reconstruction (1101 µmol m^{-2} s^{-1}) followed by the 0.2 m voxels (973 µmol m^{-2} s^{-1}) and the 1m voxels (900 µmol m^{-2} s^{-1}). The ground truth data had an average PAR of 1113 µmol m^{-2} s^{-1} and was therefore higher than any of the simulations. The general patterns of light and shade were reproduced by all simulations, but the detail was higher for the smaller voxels and even higher for the polygon reconstruction (Fig. 4). The correlation coefficient between the polygon simulation and the PAR sensor measurements was 0.92 over all sensors and time points (n = 17 496). The correlations differed substantially between

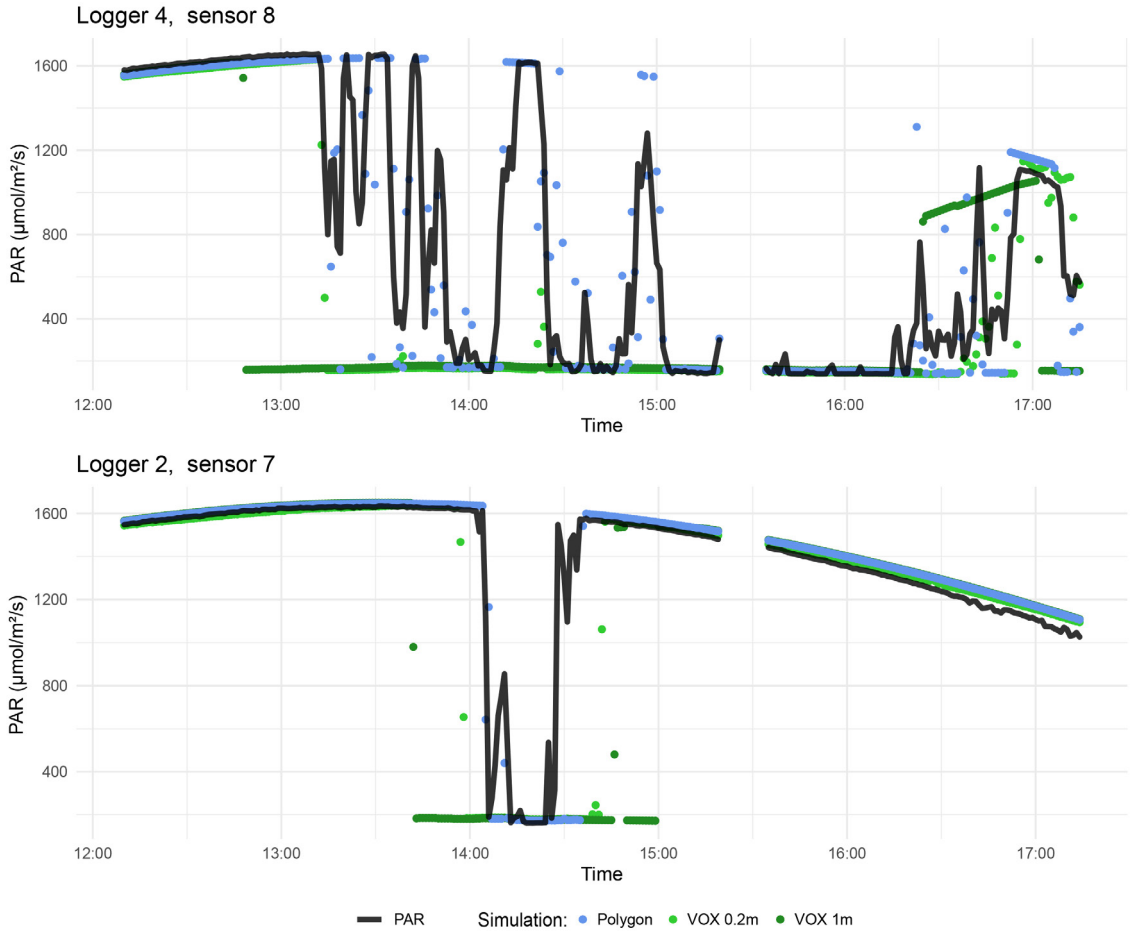

Fig. 4. Results from the radiative transfer model (LESS) for two photosynthetically active radiation (PAR) sensors next to the *Malus domestica* tree. Measured PAR values are depicted in black lines and simulated PAR values from the Polygon based simulation as blue dots, the 0.2 m voxel based simulation as light green dots and 1 m voxel based reconstruction as dark green dots.

the sensors (mean = 0.87, sd = 0.13), with the highest correlations (0.9997) for sensors which were never shaded by the tree, down to a low outlier with 0.26 for a sensor, which was nearly all time in the shade of the tree besides single peaks of sunlight due to small gaps in the tree crown. The great majority of simulated PAR values followed the pattern of the respective sensor and about the half (31 of 60) of the simulated time series exceeded correlation coefficients of 0.9 with the ground truth data and only two reached correlations lower than 0.5. The correlations for the voxel simulations were generally lower (0.2 m: 0.85; 1.0 m: 0.73). For the 1.0 m voxel simulation only 5 sensors reached correlations of 0.9 (0.2 m, n = 16) and 19 sensors were below the correlation of 0.5 (0.2 m, n = 9). Fig. 5 shows boxplots of the correlations between single sensors measured PAR values and simulated ones by LESS for the three reconstruction approaches.

To generate the geometry our polygon-based algorithm was fastest needing 4 min 41 s. To generate voxels and to calculate the PAD, AMAPvox needed 25 min 27 s for 0.2 m resolution and 19 min 51 s for 1.0 m resolution. Depending on the number of model iterations these differences in generation times might be neglectable, since this has to run only once, while for every time step or sensor placement an iteration is necessary. A single model iteration took 216.7 s for the 0.2 m voxel resolution, 7.76 s for the 1.0 m voxels, but only 5.5 s for the polygon reconstruction. All computations were performed at a workstation with an AMD Ryzen Threadripper 3960X 24-Core Processor, 256 GB RAM and a Nvidia RTX 3090 GPU with 24 GB of memory.

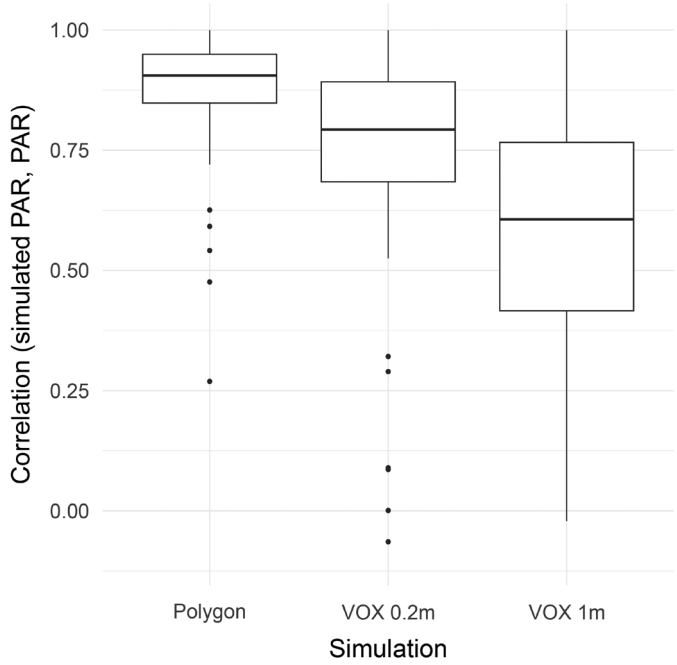

Fig. 5. Boxplots of the correlations per sensor between measured and simulated photosynthetically active radiation under and next to a tree for the three single radiative transfer simulations based on light detection and ranging (LiDAR) data reconstructed as discrete polygons, 0.2 m turbid voxels and 1 m turbid voxels.

4 Discussion

Our approach is straightforward to implement in different RTM environments such as PBRT (physically based rendering in theory and praxis, Pharr and Humphreys 2004; Biliouris et al. 2013), DART or, in this case, LESS. The direct reconstruction of the leaf and wood geometry might be a simple way to model the light interception without additional leaf-off scans (Calders et al. 2018) or additional species-specific information about leaf shape, size and distribution, but further research is need to validate it on various leaf types and species. We achieved a detailed reconstruction of the space occupied by plant material without an additional uncertainty introduced by the extend of voxel (Bittner et al. 2012; Kükenbrink et al. 2021). Contrary to these advantages, our model might suffer from occlusion in larger and denser crowns and under insufficient scanning resolution for taller canopies (Cifuentes et al. 2017; Abegg et al. 2021). This might lead to underestimations of the leaf area and sparse regions within and on top of the crowns. Limited coverage and resolution for tree parts that are at a large distance from the scanning device is inherent to all remote sensing technologies, and consequently also for the reconstruction of tree structure and optical properties (Morhart et al. 2024). This could lead to an overestimation of the solar radiation beneath big and dense crowns especially in dense mature forests. Underestimations of the transmitted radiation due to spatial limitations of the remote sensing technique are rather unrealistic since the existing shade from the lower crown part is realistically modelled. These biases are closely connected to the possible scanning devices. Phase shift scanners might especially suffer from higher occlusion due to the lack of multiple return capabilities towards the inside and the upper crown (Calders et al. 2020). Additionally, the voxel grid used to generate the shapes introduces an additional structure to the data which might also lead to artefacts, especially due to unrealistic polygon angles at

voxels which include multiple tree elements and unrealistic shapes at voxels which only contain 1 or 2 points.

There is a vast body of research tackling different reconstruction approaches for the reconstruction of the woody material (Bournez et al. 2017), which might be superior to our approach and has a relevant impact on the radiative transfer (Janoutová et al. 2019). Further research is needed to identify the optimal strategy for the wood reconstruction for leaf off and leaf on conditions and different species.

The lower correlations of the voxel-based simulations compared to the polygon reconstruction might be explained due to the lower geometrical accuracy, but also due to the uncertainties in PAD estimates from AMAPvox (Weiser et al. 2021), as the large differences in total plant area between the datasets suggest. The surprising pattern, that the total plant area was negatively related to the mean simulated PAR indicates that the clumping of the leaves and small canopy gaps contribute significantly to the overall light reaching the ground and its variability. This questions the turbid-media assumption in voxels for high resolution simulations of plant canopies.

Our approach was about 40 times faster for a single model iteration than the 0.2 m turbid voxel approach and still saves about one third of computing time compared to 1.0 m turbid voxels. This is in line with Liu et al. (2022) who found significantly higher computational demands for small scale voxels than for explicit geometry reconstructions (simulated leaves) in RTM using DART. In contrast, Janoutová et al. (2021) found that a turbid voxel approach offers advantages in computation time and memory consumption compared to explicit leaf geometries.

There is a wide range of inter-specific as well as intra-specific diversity in leaf appearance, and several studies included single species-specific leaf geometry and orientation to TLS-based leaf shape and shade modelling (Falster and Westoby 2003; Bohn Reckziegel et al. 2021). Since we tested our approach only for a single species, further research is needed to prove the overall applicability of the leaf reconstruction approach for more leaf types like needles and occlusion settings. There are no obvious obstacles why our approach should be limited to specific leaf types. Therefore, we see great potential that this approach could be used across a wide range of forest types.

We cannot exclude all uncertainties from the measurement campaign. There might be slight time offsets between the PAR-logger and the scanner clock, and we measured in a natural environment, with birds and insects, which might have cast shadows on the sensors. Even if there was nearly no wind on the measurement day, we could not ensure that there was no branch or leaf movement (Puttonen et al. 2016).

This study highlights the computational and geometrical advantages of a discrete polygon reconstruction over a voxel-based approach for radiative transfer modelling. Nevertheless, we cannot guarantee that this approach is also beneficial in respect to the radiometric accuracy of the model, since our ground truth data is not able to represent this.

Supplementary files

Metadata of research data.pdf, available at https://doi.org/10.14214/sf.24027.

Data availability

All data relevant to the study and the full R code for the reconstruction of the leaves and woody compartments can be found at our GitHub repository under open source license (Frey and Kröner 2024).

Author contributions

JF conducted the primary analyses and wrote the manuscript. ZS and CM designed and conducted the field campaign. ZS also curated and analysed the PAR data. JF and PMC conducted the radiative transfer model. TS, EL and CM gave advice on the research design. All authors read and commented on the manuscript.

Acknowledgements

This study was funded by the Deutsche Forschungsgemeinschaft (DFG, German Research Foundation) – Project FR 4404/1-1, "Making the direct link between light regime and forest biodiversity – a 3D spatially explicit modelling approach based on TLS, CNNs and ray tracing". We would further like to thank Prof. Miachel Scherer-Lorenzen of the Chair of Geobotany, Freiburg University for supplying the PAR sensors. We acknowledge support by the Open Access Publication Fund of the University of Freiburg.

References

Abegg M, Kükenbrink D, Zell J, Schaepman ME, Morsdorf F (2017) Terrestrial laser scanning for forest inventories – tree diameter distribution and scanner location impact on occlusion. Forests 8, article id 184. https://doi.org/10.3390/f8060184.

Biliouris D, Van der Zande D, Verstraeten W, Stuckens J, Muys B, Dutré P, Coppin P (2013) The importance of leaf BRDF in forest canopy bidirectional reflectance. A case study using simulated canopy architecture and PBRT ray tracing. South-Eastern Eur J Earth Observ Geomat 2: 1–17.

Bittner S, Gayler S, Biernath C, Winkler JB, Seifert S, Pretzsch H, Priesack E (2012) Evaluation of a ray-tracing canopy light model based on terrestrial laser scans. Can J Remote Sens 38: 619–628. https://doi.org/10.5589/m12-050.

Bohn Reckziegel R, Larysch E, Sheppard JP, Kahle H-P, Morhart C (2021) Modelling and comparing shading effects of 3D tree structures with virtual leaves. Remote Sensing 13, article id 532. https://doi.org/10.3390/rs13030532.

Bournez E, Landes T, Saudreau M, Kastendeuch P, Najjar G (2017) From tls point clouds to 3D models of trees: a comparison of existing algorithms for 3D tree reconstruction. Int Arch Photogramm Remote Sens Spatial Inf Sci XLII-2/W3: 113–120. https://doi.org/10.5194/isprs-archives-XLII-2-W3-113-2017.

Brunner A (1998) A light model for spatially explicit forest stand models. For Ecol Manag 107: 19–46. https://doi.org/10.1016/S0378-1127(97)00325-3.

Burchard-Levine V, Nieto H, Riaño D, Kustas WP, Migliavacca M, El-Madany TS, Nelson JA, Andreu A, Carrara A, Beringer J, Baldocchi D, Martín MP (2022) A remote sensing-based three-source energy balance model to improve global estimations of evapotranspiration in semi-arid tree-grass ecosystems. Glob Change Biol 28: 1493–1515. https://doi.org/10.1111/gcb.16002.

Calders K, Origo N, Burt A, Disney M, Nightingale J, Raumonen P, Åkerblom M, Malhi Y, Lewis P (2018) Realistic forest stand reconstruction from terrestrial LiDAR for radiative transfer modelling. Remote Sensing 10, article id 933. https://doi.org/10.3390/rs10060933.

Calders K, Adams J, Armston J, Bartholomeus H, Bauwens S, Bentley LP, Chave J, Danson FM, Demol M, Disney M, Gaulton R, Krishna Moorthy SM, Levick SR, Saarinen N, Schaaf C,

Stovall A, Terryn L, Wilkes P, Verbeeck H (2020) Terrestrial laser scanning in forest ecology: expanding the horizon. Remote Sens Environ 251, article id 112102. https://doi.org/10.1016/j.rse.2020.112102.

Chen Q, Baldocchi D, Gong P, Dawson T (2008) Modeling radiation and photosynthesis of a heterogeneous savanna woodland landscape with a hierarchy of model complexities. Agric For Meteorol 148: 1005–1020. https://doi.org/10.1016/j.agrformet.2008.01.020.

Cifuentes R, Van der Zande D, Salas C, Tits L, Farifteh J, Coppin P (2017) Modeling 3D canopy structure and transmitted PAR using terrestrial LiDAR. Can J Remote Sens 43: 124–139. https://doi.org/10.1080/07038992.2017.1286937.

Falster DS, Westoby M (2003) Leaf size and angle vary widely across species: what consequences for light interception? New Phytol 158: 509–525. https://doi.org/10.1046/j.1469-8137.2003.00765.x.

Feret J-B, François C, Asner GP, Gitelson AA, Martin RE, Bidel LPR, Ustin SL, le Maire G, Jacquemoud S (2008) PROSPECT-4 and 5: advances in the leaf optical properties model separating photosynthetic pigments. Remote Sens Environ 112: 3030–3043. https://doi.org/10.1016/j.rse.2008.02.012.

Forrester DI, Rodenfels P, Haase J, Härdtle W, Leppert KN, Niklaus PA, von Oheimb G, Scherer-Lorenzen M, Bauhus J (2019) Tree-species interactions increase light absorption and growth in Chinese subtropical mixed-species plantations. Oecologia 191: 421–432. https://doi.org/10.1007/s00442-019-04495-w.

Frey J, Kröner K (2024) JulFrey/dotshadow: Dotshadow – create a polygon reconstruction of vegetation from terrestrail LiDAR data for radiative transfer modelling. Zenodo. https://doi.org/10.5281/zenodo.14204435.

Gastellu-Etchegorry J-P, Grau E, Lauret N (2012) DART: a 3D model for remote sensing images and radiative budget of earth surfaces. In: Alexandru C (ed) Modeling and Simulation in Engineering. InTech, pp 29–68. https://doi.org/10.5772/31315.

Gastellu-Etchegorry J-P, Lauret N, Yin T, Landier L, Kallel A, Malenovsky Z, Bitar AA, Aval J, Benhmida S, Qi J, Medjdoub G, Guilleux J, Chavanon E, Cook B, Morton D, Chrysoulakis N, Mitraka Z (2017) DART: recent advances in remote sensing data modeling with atmosphere, polarization, and chlorophyll fluorescence. IEEE J Sel Top Appl 10: 2640–2649. https://doi.org/10.1109/JSTARS.2017.2685528.

Green SR, Vogeler I, Clothier BE, Mills TM, Dijssel CVD (2003) Modelling water uptake by a mature apple tree. Soil Res 41: 365–380. https://doi.org/10.1071/SR02129.

Huston MA, Marland G (2003) Carbon management and biodiversity. J. Environ. Manag 67: 77–86. https://doi.org/10.1016/S0301-4797(02)00190-1.

Janoutová R, Homolová L, Malenovský Z, Hanuš J, Lauret N, Gastellu-Etchegorry J-P (2019) Influence of 3D spruce tree representation on accuracy of airborne and satellite forest reflectance simulated in DART. Forests 10, article id 292. https://doi.org/10.3390/f10030292.

Janoutová R, Homolová L, Novotný J, Navrátilová B, Pikl M, Malenovský Z (2021) Detailed reconstruction of trees from terrestrial laser scans for remote sensing and radiative transfer modelling applications. In Silico Plants 3, article id diab026. https://doi.org/10.1093/insilicoplants/diab026.

Kattge J, Bönisch G, Díaz S, Lavorel S, Prentice IC, Leadley P, Tautenhahn S, Werner GDA, Aakala T, Abedi M, Acosta ATR, Adamidis GC, Adamson K, Aiba M, Albert CH, Alcántara JM, Alcázar C C, Aleixo I, Ali H, Amiaud B, Ammer C, et al. (2020) TRY plant trait database – enhanced coverage and open access. Glob Change Biol 26: 119–188. https://doi.org/10.1111/gcb.14904.

Kelley D, Richards C (2022) oce: analysis of oceanographic data.

Kükenbrink D, Hueni A, Schneider FD, Damm A, Gastellu-Etchegorry J-P, Schaepman ME, Morsdorf F (2019) Mapping the irradiance field of a single tree: quantifying vegetation-induced adjacency effects. IEEE T Geosci Remote 57: 4994–5011. https://doi.org/10.1109/TGRS.2019.2895211.

Kükenbrink D, Schneider FD, Schmid B, Gastellu-Etchegorry J-P, Schaepman ME, Morsdorf F (2021) Modelling of three-dimensional, diurnal light extinction in two contrasting forests. Agric For Meteorol 296, article id 108230. https://doi.org/10.1016/j.agrformet.2020.108230.

Latimer CE, Zuckerberg B (2017) Forest fragmentation alters winter microclimates and microrefugia in human-modified landscapes. Ecography 40: 158–170. https://doi.org/10.1111/ecog.02551.

Leuchner M, Hertel C, Rötzer T, Seifert T, Weigt R, Werner H, Menzel A (2012) Solar radiation as a driver for growth and competition in forest stands. In: Matyssek R, Schnyder H, Oßwald W, Ernst D, Munch JC, Pretzsch H (eds) Growth and defence in plants: resource allocation at multiple scales. Springer, Berlin, Heidelberg, pp 175–191. https://doi.org/10.1007/978-3-642-30645-7_8.

Li W, Guo Q, Tao S, Su Y (2018) VBRT: a novel voxel-based radiative transfer model for heterogeneous three-dimensional forest scenes. Remote Sens Environ 206: 318–335. https://doi.org/10.1016/j.rse.2017.12.043.

Ligot G, Balandier P, Courbaud B, Claessens H (2014) Forest radiative transfer models: which approach for which application? Can J For Res 44: 391–403. https://doi.org/10.1139/cjfr-2013-0494.

Lintunen A, Kaitaniemi P, Perttunen J, Sievänen R (2013) Analysing species-specific light transmission and related crown characteristics of *Pinus sylvestris* and *Betula pendula* using a shoot-level 3D model. Can J For Res 43: 929–938. https://doi.org/10.1139/cjfr-2013-0178.

Liu C, Calders K, Meunier F, Gastellu-Etchegorry JP, Nightingale J, Disney M, Origo N, Woodgate W, Verbeeck H (2022) Implications of 3D forest stand reconstruction methods for radiative transfer modeling: a case study in the temperate deciduous forest. J Geophys Res Atmos 127, article id e2021JD036175. https://doi.org/10.1029/2021JD036175.

Magney TS, Eitel JUH, Griffin KL, Boelman NT, Greaves HE, Prager CM, Logan BA, Zheng G, Ma L, Fortin EA, Oliver RY, Vierling LA (2016) LiDAR canopy radiation model reveals patterns of photosynthetic partitioning in an Arctic shrub. Agric For Meteorol 221: 78–93. https://doi.org/10.1016/j.agrformet.2016.02.007.

Malenovský Z, Regaieg O, Yin T, Lauret N, Guilleux J, Chavanon E, Duran N, Janoutová R, Delavois A, Meynier J, Medjdoub G, Yang P, van der Tol C, Morton D, Cook BD, Gastellu-Etchegorry J-P (2021) Discrete anisotropic radiative transfer modelling of solar-induced chlorophyll fluorescence: structural impacts in geometrically explicit vegetation canopies. Remote Sens Environ 263, article id 112564. https://doi.org/10.1016/j.rse.2021.112564.

Malhi Y, Phillips OL, Laurance WF (2004) Forest-climate interactions in fragmented tropical landscapes. Philos Trans R Soc Lond B Biol Sci 359: 345–352. https://doi.org/10.1098/rstb.2003.1430.

Mederer D, Feilhauer H, Cherif E, Berger K, Hank TB, Kovach KR, Dao PD, Lu B, Townsend PA, Kattenborn T (2025) Plant trait retrieval from hyperspectral data: collective efforts in scientific data curation outperform simulated data derived from the PROSAIL model. ISPRS J Photogramm Remote Sens 15, article id 100080. https://doi.org/10.1016/j.ophoto.2024.100080.

Morhart C, Schindler Z, Frey J, Sheppard JP, Calders K, Disney M, Morsdorf F, Raumonen P, Seifert T (2024) Limitations of estimating branch volume from terrestrial laser scanning. Eur J Forest Res 143: 687–702. https://doi.org/10.1007/s10342-023-01651-z.

Ni-Meister W, Gao H (2011) Assessing the impacts of vegetation heterogeneity on energy fluxes

and snowmelt in boreal forests. J Plant Ecol 4: 37–47. https://doi.org/10.1093/jpe/rtr004.

Pacheco-Labrador J, Migliavacca M, Ma X, Mahecha MD, Carvalhais N, Weber U, Benavides R, Bouriaud O, Barnoaiea I, Coomes DA, Bohn FJ, Kraemer G, Heiden U, Huth A, Wirth C (2022) Challenging the link between functional and spectral diversity with radiative transfer modeling and data. Remote Sens Environ 280, article id 113170. https://doi.org/10.1016/j.rse.2022.113170.

Pharr M, Humphreys G (eds) (2004) Physically based rendering. From theory to implementation. Morgan Kaufmann, Burlington.

Porcar-Castell A, Malenovský Z, Magney T, Van Wittenberghe S, Fernández-Marín B, Maignan F, Zhang Y, Maseyk K, Atherton J, Albert LP, Robson TM, Zhao F, Garcia-Plazaola J-I, Ensminger I, Rajewicz PA, Grebe S, Tikkanen M, Kellner JR, Ihalainen JA, Rascher U, Logan B (2021) Chlorophyll a fluorescence illuminates a path connecting plant molecular biology to Earth-system science. Nat Plants 7: 998–1009. https://doi.org/10.1038/s41477-021-00980-4.

Puttonen E, Briese C, Mandlburger G, Wieser M, Pfennigbauer M, Zlinszky A, Pfeifer N (2016) Quantification of overnight movement of birch (*Betula pendula*) branches and foliage with short interval terrestrial laser scanning. Front Plant Sci 7, article id 222. https://doi.org/10.3389/fpls.2016.00222.

Qi J, Xie D, Yin T, Yan G, Gastellu-Etchegorry J-P, Li L, Zhang W, Mu X, Norford LK (2019) LESS: LargE-Scale remote sensing data and image simulation framework over heterogeneous 3D scenes. Remote Sens Environ 221: 695–706. https://doi.org/10.1016/j.rse.2018.11.036.

R Core Team (2024) R: a language and environment for statistical computing. R Foundation for Statistical Computing, Vienna, Austria.

Regaieg O, Yin T, Malenovský Z, Cook BD, Morton DC, Gastellu-Etchegorry J-P (2021) Assessing impacts of canopy 3D structure on chlorophyll fluorescence radiance and radiative budget of deciduous forest stands using DART. Remote Sens Environ 265, article id 112673. https://doi.org/10.1016/j.rse.2021.112673.

Rosskopf E, Morhart C, Nahm M (2017) Modelling shadow using 3D tree models in high spatial and temporal resolution. Remote Sensing 9, article id 719. https://doi.org/10.3390/rs9070719.

Rötzer T, Seifert T, Gayler S, Priesack E, Pretzsch H (2012) Effects of stress and defence allocation on tree growth: simulation results at the individual and stand level. In: Matyssek R, Schnyder H, Oßwald W, Ernst D, Munch JC, Pretzsch H (eds) Growth and defence in plants: resource allocation at multiple scales. Springer, Berlin, Heidelberg, pp 401–432. https://doi.org/10.1007/978-3-642-30645-7_18.

Schneider FD, Leiterer R, Morsdorf F, Gastellu-Etchegorry J-P, Lauret N, Pfeifer N, Schaepman ME (2014) Simulating imaging spectrometer data: 3D forest modeling based on LiDAR and in situ data. Remote Sens Environ 152: 235–250. https://doi.org/10.1016/j.rse.2014.06.015.

Serbin SP (2013) Rprospect: R functions for running PROSPECT family of leaf radiative transfer models. https://rdrr.io/github/serbinsh/R-PROSPECT/.

Van Cleemput E, Roberts DA, Honnay O, Somers B (2019) A novel procedure for measuring functional traits of herbaceous species through field spectroscopy. Methods Ecol Evol 10: 1332–1338. https://doi.org/10.1111/2041-210X.13237.

Van der Zande D, Stuckens J, Verstraeten WW, Muys B, Coppin P (2010) Assessment of light environment variability in broadleaved forest canopies using terrestrial laser scanning. Remote Sens 2: 1564–1574. https://doi.org/10.3390/rs2061564.

Van der Zande D, Stuckens J, Verstraeten WW, Mereu S, Muys B, Coppin P (2011) 3D modeling of light interception in heterogeneous forest canopies using ground-based LiDAR data. Int J Appl Earth Obs Geoin 13: 792–800. https://doi.org/10.1016/j.jag.2011.05.005.

Vezy R, Christina M, Roupsard O, Nouvellon Y, Duursma R, Medlyn B, Soma M, Charbonnier F,

Blitz-Frayret C, Stape J-L, Laclau J-P, de Melo Virginio Filho E, Bonnefond J-M, Rapidel B, Do FC, Rocheteau A, Picart D, Borgonovo C, Loustau D, le Maire G (2018) Measuring and modelling energy partitioning in canopies of varying complexity using MAESPA model. Agric For Meteorol 253–254: 203–217. https://doi.org/10.1016/j.agrformet.2018.02.005.

Vincent G, Antin C, Laurans M, Heurtebize J, Durrieu S, Lavalley C, Dauzat J (2017) Mapping plant area index of tropical evergreen forest by airborne laser scanning. A cross-validation study using LAI2200 optical sensor. Remote Sens Environ 198: 254–266. https://doi.org/10.1016/j.rse.2017.05.034.

Wang Y, Frankenberg C (2022) On the impact of canopy model complexity on simulated carbon, water, and solar-induced chlorophyll fluorescence fluxes. Biogeosciences 19: 29–45. https://doi.org/10.5194/bg-19-29-2022.

Wang YP, Jarvis PG (1990) Description and validation of an array model – MAESTRO. Agric For Meteorol 51: 257–280. https://doi.org/10.1016/0168-1923(90)90112-J.

Weiser H, Winiwarter L, Anders K, Fassnacht FE, Höfle B (2021) Opaque voxel-based tree models for virtual laser scanning in forestry applications. Remote Sens Environ 265, article id 112641. https://doi.org/10.1016/j.rse.2021.112641.

Widlowski J-L, Côté J-F, Béland M (2014) Abstract tree crowns in 3D radiative transfer models: impact on simulated open-canopy reflectances. Remote Sens Environ 142: 155–175. https://doi.org/10.1016/j.rse.2013.11.016.

Xie D, Wang X, Qi J, Chen Y, Mu X, Zhang W, Yan G (2018) Reconstruction of single tree with leaves based on terrestrial LiDAR point cloud data. Remote Sensing 10, article id 686. https://doi.org/10.3390/rs10050686.

Total of 58 references.